



Early Cognitive Impairment Behind Nigrostriatal Circuit Neurotoxicity: Are Astrocytes Involved?

ASN Neuro
Volume 12: 1–17
© The Author(s) 2020
Article reuse guidelines:
sagepub.com/journals-permissions
DOI: 10.1177/1759091420925977
journals.sagepub.com/home/asn


Macarena L. Herrera^{1,2}, Romina Deza-Ponzio¹, Marisa S. Gherzi¹, Emilce A. de la Villarmois¹, Miriam B. Virgolini¹, Mariela F. Pérez¹, Victor A. Molina¹, María J. Bellini^{2,*}, and Claudia B. Hereñú^{1,*} 

Abstract

Cognitive dysfunction is one of the most severe nonmotor symptoms of nigrostriatal impairment. This occurs as a result of profound functional and morphological changes of different neuronal circuits, including modifications in the plasticity and architecture of hippocampal synapses. Such alterations can be implicated in the genesis and progression of dementia associated with neurodegenerative diseases including Parkinson-like symptoms. There are few studies regarding cognitive changes in nigrostriatal animal models. The aim of this study was to characterize the onset of memory deficit after induction of neurotoxicity with 6-hydroxydopamine (6-OHDA) and its correlation with hippocampal dysfunction. For this, we bilaterally microinjected 6-OHDA in dorsolateral Caudate-Putamen unit (CPu) and then, animals were tested weekly for working memory, spatial short-term memory, and motor performance. We evaluated tyrosine hydroxylase (TH) as a dopamine marker, aldehyde dehydrogenase 2 (ALDH2), a mitochondria detoxification enzyme and astrocyte glial fibrillar acid protein (GFAP) an immunoreactivity marker involved in different areas: CPu, substantia nigra, prefrontal cortex, and hippocampus. We observed a specific prefrontal cortex and nigrostriatal pathway TH reduction while ALDH2 showed a decrease-positive area in all the studied regions. Moreover, GFAP showed a specific CPu decrease and hippocampus increase of positively stained area on the third week after toxicity. We also evaluated the threshold to induce long-term potentiation in hippocampal excitability. Our findings showed that reduced hippocampal synaptic transmission was accompanied by deficits in memory processes, without affecting motor performance on the third-week post 6-OHDA administration. Our results suggest that 3 weeks after neurotoxic administration, astrocytes and ALDH2 mitochondrial enzyme modifications participate in altering the properties that negatively affect hippocampal function and consequently cognitive behavior.

Keywords

neurotoxicity, 6-OHDA, synaptic plasticity, cognitive dysfunction, astrocytes, ALDH2

Received December 18, 2019; Revised March 29, 2020; Accepted for publication April 1, 2020

Cognitive dysfunction is one of the most severe nonmotor symptoms (NMS) of nigrostriatal impairment, leading to a negative impact associated with Parkinson's Disease (PD) patients' quality of life and increased caregiver burden (Ehgoetz Martens and Lewis, 2017). The focus on cognitive impairment in neurodegenerative diseases is shifting from end dementia stage to earlier stages of impairment (Weintraub et al., 2018). The affected areas are involved in executive, attentional and visuospatial domains, as well as memory functions. It has been observed that the spectrum of cognitive impairment can range from normal to mild cognitive impairment (MCI) to moderate and even severe Parkinson's disease with dementia (PDD; Aarsland

¹Instituto de Farmacología Experimental de Córdoba (IFEC-CONICET), Departamento de Farmacología, Facultad de Ciencias Químicas, Universidad Nacional de Córdoba

²Instituto de Investigaciones Bioquímicas de La Plata (INIBIOLP-CONICET), Facultad de Ciencias Médicas, Universidad Nacional de La Plata, Buenos Aires, Argentina

*These authors contributed equally to this work.

Corresponding Authors:

Claudia B. Hereñú, Instituto de Farmacología Experimental de Córdoba (IFEC-CONICET), Departamento de Farmacología, Facultad de Ciencias Químicas, Universidad Nacional de Córdoba, Haya de la Torre S/N, esquina Medina Allende, Edificio Nuevo de Ciencias I Ciudad Universitaria, Córdoba CP500, Argentina.

Email: cherenu@fcq.unc.edu.ar

María J. Bellini, Instituto de Investigaciones Bioquímicas de La Plata (INIBIOLP-CONICET), Universidad Nacional de La Plata, Facultad de Ciencias Médicas, Av. 60 s/n, La Plata CP1900, Buenos Aires, Argentina.

Email: mariajosebellini@yahoo.com



et al., 2017). Approximately 25% of nondemented PD patients have MCI, while up to 80% of all PD patients will eventually develop dementia (Aarsland and Kurz, 2010). A great heterogeneity among cognitive deficits, characterized by subtle changes difficult to detect and diagnose, was reported (Schapira et al., 2017). These PD-associated cognitive changes are very difficult to find in current PD animal models, particularly when these impairments appear in premotor stage, before the onset of motor deficits. Emerging data suggest that dopamine release in the hippocampus could contribute to the synaptic plasticity required for updating learning and memory (Broussard et al., 2016). Any failure to connect these circuits could be involved in the genesis and progression of dementia as well as in another neuropsychiatric aspects of the nigrostriatal dysfunction circuit (Calabresi et al., 2013). In this context, the development of an experimental animal model of Parkinsonism that allows delving into the cognitive deterioration process would constitute a significant contribution to the understanding of the process.

In addition to neuronal circuits, glial cells and brain detoxification processes are fundamental for brain function. Astrocytes take part in the maintenance of neuronal functions through thousands of small processes that surround neuronal processes (Bazzari and Parri, 2019). Among others, they aid neuronal transmission (Allen, 2014), participate in the recycling of neurotransmitters and the uptake of circulating lipids and glucose from the blood, metabolizing them and supplying the products to neurons as an energy source (van Deijk et al., 2017). The aging process is associated with a reduction of brain responses to injury, mitochondrial-derived energy production and a decline in neuronal and astroglial functions. The impairment and loss of astrocytic mitochondria leads to oxidative stress/damage, diminished adenosine triphosphate levels, excessive radical production, and dysregulated apoptosis. These dysfunctions are part of the etiology of many age-related human diseases including neurotoxicity and neurodegenerative disorders (Herrera et al., 2019).

The neurotoxin 6-hydroxydopamine (6-OHDA) has affinity for catecholamines and is taken up by the dopamine transporter. Depending on the administration site, 6-OHDA allows selective damage to dopaminergic and noradrenergic neurons of different brain areas, mainly in the nigrostriatal pathway in rats and mice (Commins et al., 1989). The formation of reactive oxygen species (ROS) by the auto-oxidation of 6-OHDA is considered the main molecular mechanism of action, although a direct inhibition of the mitochondrial respiratory chain complex I has been also reported (Rodríguez-Pallares et al., 2007). Thus, by blocking mitochondrial complex I and thereby nicotinamide adenine dinucleotide (NAD⁺) generation, 6-OHDA could decrease intracellular ALDH

activity indirectly. NAD is a required cofactor for ALDH, the key component of toxic DA metabolites metabolism, particularly 3,4-dihydroxyphenylacetaldehyde (DOPAL), which is involved in PD etiology (Deza-Ponzio et al., 2018).

Based on the early occurrence of cognitive dysfunction in nigrostriatal circuit impairment and the effect of striatal dopamine depletion on cognition, we decided to test the hypothesis that these deficits result from the dysfunction of interconnected systems, including the Caudate-Putamen unit (CPu) and the hippocampus. The fact that the appearance of NMS in Parkinsonian patients correlates not only to the progressive depletion of DA but also to the concomitant degeneration of noradrenergic, serotonergic, and cholinergic systems (Braak et al., 2003) prompted us to use a neurotoxic animal model induced by 6-OHDA to characterize the onset of memory dysfunction before motor alterations and its correlation with hippocampal electrophysiological recordings. We found that the injection of 20 µg of neurotoxin per hemisphere promoted cognitive deficits. Remarkably, these results correlate with striatal dopamine depletion and long-term potentiation (LTP) impairments in hippocampus. Moreover, as part of our study, we also explored the hypothesis that decreased neuronal and synaptic function in the 6-OHDA neurotoxic model is associated to altered properties of astrocytes and ALDH2 dysfunction that negatively affect neurons and behavior.

Materials and Methods

Animals

Male adult Wistar rats (280–320 g; ~8 weeks old; $n = 125$) obtained from the Department of Pharmacology facility (National University of Cordoba, Argentina), were used in this study. Animals were maintained in a controlled room temperature (21°C–23°C) in groups of three animals per Plexiglas cage, with 12:12-h light/dark cycle receiving food and water ad libitum through all the experiment. All procedures were performed in accordance with the NIH Guide for the Care and Use of Laboratory Animals, as well as by the Animal Care and Use Committee CICUAL, Argentina (0030162/2017). Special care was taken to minimize suffering and to reduce the number of animals used to the minimal required for statistical accuracy.

Experimental Protocol

Animals were randomly divided into two experimental groups: (a) SHAM group (injected with 4 µL of ascorbic saline as vehicle solution) and (b) 6-OHDA group (injected with 4 µL of neurotoxic). The day of the stereotaxic lesion was considered day 0. To detect cognitive

impairments, we performed cognitive and motor tests throughout four different stages (at weeks 1, 2, 3, and 4) in independent groups of rats, each animal received only one memory task, followed by motor tests. After behavioral evaluation, each set of animals were sacrificed. We detected early cognitive deficits, without motor alterations, 3 weeks after day 0. Therefore, at 3 weeks from neurotoxicity, we performed specific locomotor activity (induced by amphetamine administration) and a hippocampal-dependent memory test (using novel location recognition [NLR] and modified Y-Maze) to support these observations. These animals were sacrificed and biochemical and electrophysiological assays were carried out. At 4 weeks, it was not possible to evaluate a cognitive performance, since half of 6-OHDA rats were discarded according to the selection criteria of the Y-Maze test (detailed in Cognitive tests section; Figure 1).

Drugs

6-OHDA (Sigma Chemicals Co., St. Louis, MO, USA) was dissolved in saline with L-ascorbic acid (0.02%, Sigma Chemicals Co.) and administered by intrastriatal injection. D-amphetamine sulfate (Amph 0.5 mg/kg, Sigma Chemical Co.) was dissolved in 0.9% saline and administered intraperitoneal (i.p.) on the third and fourth weeks of neurotoxicity. All drugs were prepared freshly before the beginning of each experiment.

Surgery

To produce an early model of Parkinsonism with a partial lesion of the dopaminergic nigrostriatal pathway, the doses, and points of injections were previously selected according to a pilot study following reports of Kirik et al., (1998) and Matheus et al. (2016). The criteria to determine the dose and points of injections were considered following the good health of the animal (motor recuperation after surgery and loss of weight, data not shown). We determined bilateral microinjection in dorsolateral striatum (CPu) corresponding to the coordinates from Paxinos et al. (2009; anteroposterior [AP]: +0.2 mm, mediolateral [ML]: ± 3.5 mm, dorsoventral [DV]: -4.8 mm from Bregma) with either 2 μ L of the vehicle per hemisphere (saline solution with 0.02% ascorbic acid) or 2 μ L of 6-OHDA per hemisphere (dose of 10 μ g/ μ L) at a flow rate of 0.5 μ L/min. A total of 40 μ g of neurotoxic were used per animal. Drug administration was performed employing a 30G injector connected by polyethylene tubing to a 10 μ L Hamilton syringe. An infusion pump was employed to ensure correct volume and flow. Following microinjection, the cannula was left in place for 2 min before being retracted, to allow complete diffusion of the drug. Stereotaxic surgeries were performed under ketamine (55 mg/kg)/xylazine (11 mg/kg) i.p. anesthesia and antibiotic administration.

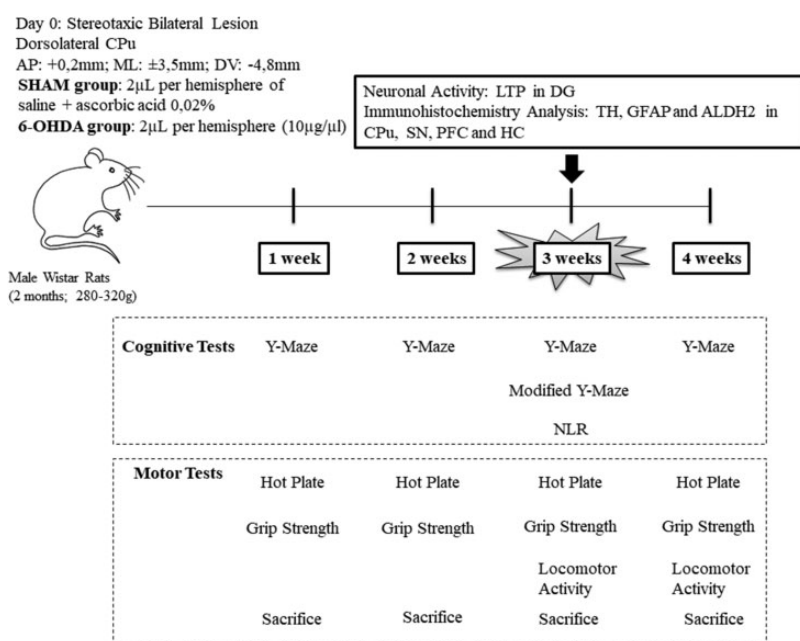


Figure 1. Experimental Protocol Design. Schematic Representation of the Experimental Protocol. Behavioral tests evaluation in rats injected with 6-hydroxydopamine (6-OHDA) or vehicle (SHAM) through four different weeks in independent groups. Only rats at 3 weeks after 6-OHDA were sacrificed for neuronal activity analysis through long-term potentiation (LTP) recordings in dentate gyrus (DG) and for immunohistochemistry analysis of tyrosine hydroxylase (TH) enzyme, astrocyte immunoreactivity (GFAP) and mitochondrial enzyme ALDH2 in the caudate-putamen unit (CPu), substantia nigra (SN), prefrontal cortex (PFC) and hippocampus (CAI).

Behavioral Tests

Approximately 125 animals were tested to complete the set of experiments throughout 2 years of work (all year round). From these experimental animals, we used 52 animals at third week of neurotoxicity. In Supplemental Material, we added 73 animals of first, second, and fourth weeks of neurotoxicity, for statistical comparisons. All tests were carried out from 10:00 to 16:00 in the same low-intensity light room and analyzed by the same experimenter. The rats were left inside the experimental room 40 min before the beginning of the tests for habituation and to avoid stressors. Trials were monitored through a video camera positioned above each arena. The videos were later analyzed with Ethowatcher[®] software (Crispim Junior et al., 2012) by a trained observer. All the arenas were cleaned with 70% ethanol to remove odor cues between each animal tested. We employed independent animal groups for each trial and time stage. Each cohort was divided, in similar amounts, in two experimental groups: 6-OHDA and SHAM and were run simultaneously on the same day under the same room conditions.

Cognitive tests. At 3 weeks post lesion, different sets of animals were tested in three spatial memory paradigms: spontaneous exploration of three places (working memory), recognition of a new place, and recognition of novel location of a familiar object (short-term memory).

Y-Maze Test. Animals were tested for working memory by Y-maze test to explore areas that have not been previously explored. The Y-maze apparatus has three wooden branches (50 cm long, 10 cm wide, and 20 cm high) covered with impermeable Formica elevated 50 cm above the floor (Figure 2A). During the 5-min test, rats were placed at the end of Branch 1 facing the center, and they could choose between Branches 2 and 3. Entry into a branch was defined as placement of the four paws into the branch, and an alternation was defined as triplet of consecutive entries to different branches. Animals that do not reach the criteria—(a) minimum of entries five and (b) 2 min without a new movement or entry—were excluded.

Modified Y-Maze Test. We performed a Y-maze variant, in the same apparatus, for short-term memory evaluation. The test consisted of two trials: (a) training and (b) test (5 min each) separated by an inter-trial interval of 120 min. During the training trial, rats were placed in the start branch, facing the center. Exploration occurred between Branch 1 and Branch 2. Branch 3 was blocked by a removable door (novel arm). In the test trial, the novel arm was opened and the exploration occurred

between the three arms (Figure 2D). We recorded: total time exploration between trials and number of entries.

Novel Location Recognition Test. NLR test was adapted from Sarkisyan and Hedlund (2009). On Day 1, rats were individually habituated for 5 min to a 60 cm × 60 cm × 40 cm square open field (OF) with black Plexiglas walls. On Day 2, the rats were trained in two consecutive 5-min familiarization trials (with an inter-trial rest interval of 90 min) and tested for NLR. Three similar nontoxic plastic objects were placed, during familiarization trials, in the corners of the OF (SW = southwest, NW = northwest, SE = southeast) at a considerable distance from the arena walls and filled with plaster to prevent rats from moving the objects during testing. An individual rat was placed in the center of the field facing the same direction in each trial and was allowed to explore for 5 min. The objects locations were kept between trials and animals. After two familiarization trials, rats were submitted to a NLR test, in which one of the familiar objects was moved to an adjacent vacant position of the arena (SE to NE = northeast). The same object was moved to the same new location for every rat tested. All trials were videotaped and the time spent exploring each object was determined (Figure 2I). We considered *exploration* as approaching the object nose-first within 2 to 4 cm. Location novelty recognition was calculated as the difference between the percent time spent exploring the object in the new location and the media of the percent times exploring the object in its original location during the two familiarization trials.

Motor Tests. One day after cognitive evaluation, animals were submitted to different motor activity tests to correlate cognitive dysfunction in the absence of motor deficits. We analyzed strength, sensitive-motor performance, and amphetamine-induced locomotor activity.

Grip Strength. The time the animal remained suspended holding its own weight was recorded according to Nishida et al. (2011). We placed the animal briefly on a horizontal wire mesh pole located 70 cm from the floor (with a cushion mattress as fall protection). Immediately, the pole was gently rotated downwards. Trials began when each animal was suspended holding on its four legs and ended when the rat fell off the pole, and latency was recorded (Figure 3A). Animals were tested twice consecutively (with a 5-min inter-trial rest interval) and the media of these trials was used.

Hot Plate Test. To assess sensitive-motor dysfunction we placed animals, individually, on a heated surface (54°C) positioned over a black box (33 cm × 25 cm × 33 cm; Figure 3C). The time taken to shake or lick its paws

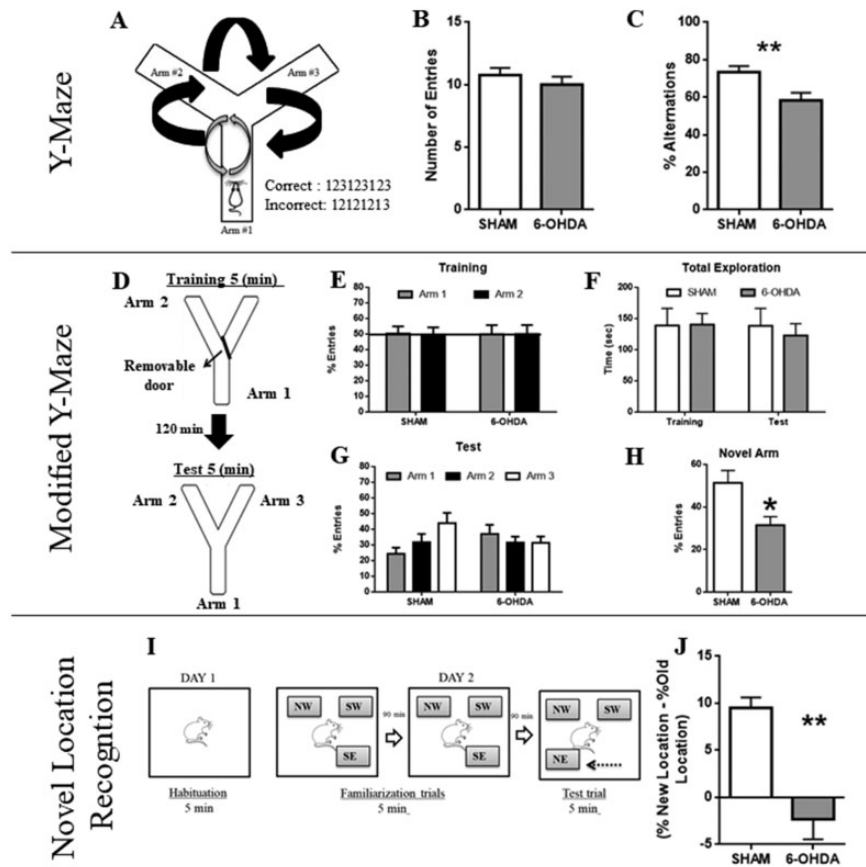


Figure 2. Cognitive Tests. Working Memory in the Y-Maze Task. A: Schematic representation of Y-Maze apparatus with three arms. Black arrows indicate a correct circuit of alternations. Gray arrows indicate an incorrect circuit of alternations. B: The total number of arm entries for the two experimental groups at 3 weeks of neurotoxicity. C: Percentage of alternations in this task; at 3 weeks post-lesion the number of entries remains intact but a decrease in the percentage of alternations was observed. $N = 13$ (SHAM) versus $N = 15$ (6-OHDA). Values are the mean \pm SEM; (** $p < .01$). Spatial short-term memory in the Modified Y-Maze task. D: Schematic representation of Y-Maze apparatus with three arms for training and test sessions. E: Percent of arms entries during training session. F: Total time of exploration: both groups evidence the same time of total exploration of the maze. G: Test Trial: There is no significant difference among the exploration in 6-OHDA animals in the three arms. H: Number of Entries into the novel arm: SHAM animals show a significant difference of entries into the novel arm when compared to 6-OHDA. $N = 7$ (SHAM) versus $N = 5$ (6-OHDA). Values are the mean \pm SEM. *Different from SHAM group ($p < .05$). Novel Location Recognition task at 3 weeks of neurotoxicity. I: Schematic representation of the trial. Day 1: one habituation session of 5 min (without objects). Day 2: two familiarization trials of 5 min each (with a rest inter-trial interval of 90 min); NW = northwest; SW = southwest; SE = southeast. Then, in the test trial (5 min) the SE object was moved to the position NE = northeast. J: Novel location exploration is ordered by the difference in the percentage of exploration of the same object in the new and old location, respectively. $N = 7$ (SHAM) versus $N = 5$ (6-OHDA). Values are the mean \pm SEM. **Different from SHAM group ($p < .01$).

was considered as the first sign of nociception. A cutoff period of 120 s was set to avoid animal thermal injury (Occhieppo et al., 2017). We considered three variables (a) time taken to feel the stimulus (Initial Time), (b) time taken to escape from the stimulus (Final Time), and (c) the difference between final time and the initial time (Reaction Time).

Locomotor Activity Test. In unilateral models, using Hemiparkinsonian rats, tests to assess motor impairment use rotational studies induced with certain drugs (Mokry, 1995) in different experimental periods of time. Tests that

allow quantification of spontaneous motor or sensorimotor functions are very useful to evaluate nigrostriatal neurotoxicity circuits. Among them, amphetamines (AMPH; d-amphetamine or meth-amphetamine) act presynaptically to stimulate DA release and/or block DA reuptake. So the amphetamine test, a dopamine stimulant drug, reflects the imbalance in DA release between the denervated and the nondenervated striata (Björklund and Dunnett, 2019). Animals exhibited ipsilateral rotations when challenged with D-amphetamine. Apomorphine administration caused contralateral circling behavior (Yuan et al., 2005; Sindhu et al., 2006; Boix et al., 2015). To sort out the lack

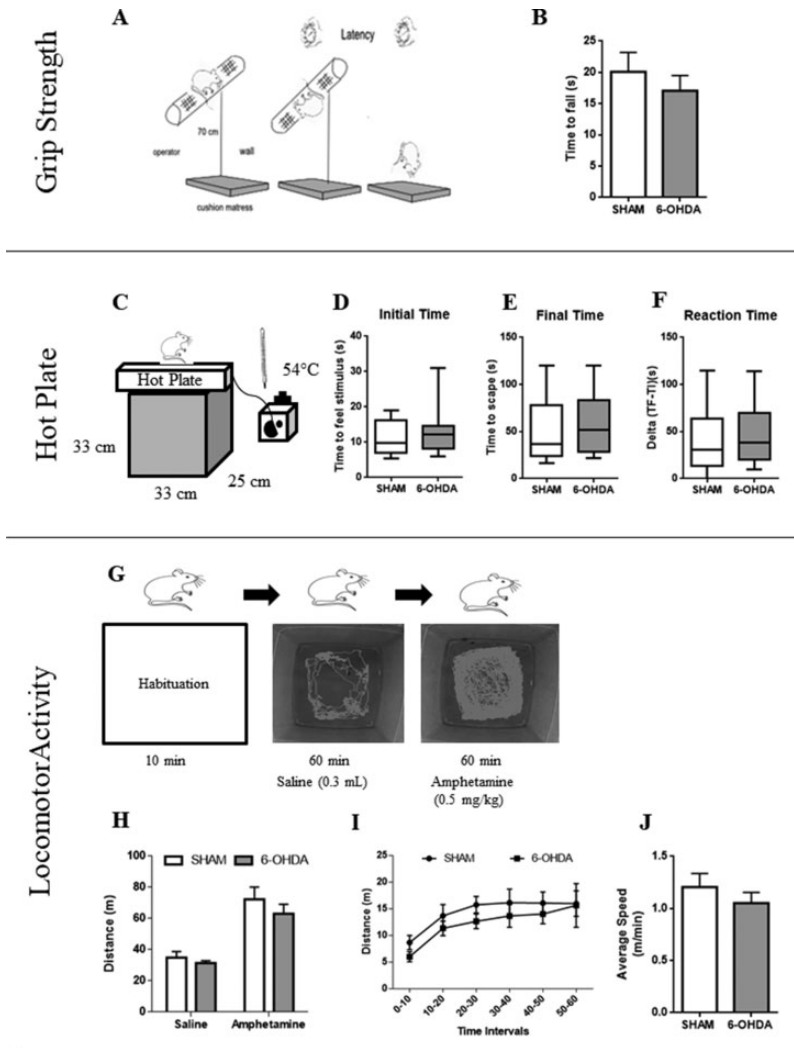


Figure 3. Motor Tests. Grip strength task. A: Schematic representation of the trial. B: The panel shows the resistance time of rats to fall from a horizontal pole wire mesh. Time represents the resistance to fall. $N = 11$ (SHAM) versus $N = 11$ (6-OHDA). Values are the mean \pm SEM. Nociceptive perception in the hot plate task. C: Schematic representation of the experimental protocol. D: Initial time is defined as the latency for the first sign of nociception. E: Final Time is defined as the latency for escapes the stimuli. F: Reaction time is defined as the difference between final and initial times. $N = 17$ (SHAM) versus $N = 17$ (6-OHDA). Values are the mean \pm SEM. Locomotor activity task induced by amphetamine administration. G: Schematic representation of the experimental protocol. H: Comparisons between saline and amphetamine administration for both experimental groups. I: Analysis of distance walked in period of 10 min. J: Average speed performed in SHAM and 6-OHDA rats. $N = 9$ (SHAM) versus $N = 9$ (6-OHDA). Values are the mean \pm SEM.

of rotational analysis in this bilateral model, the specific motor function was assessed by pharmacological induction (Vanderschuren et al., 1999). However, we used a lower dose (0.5 mg/kg) to avoid sensitization but enough to enhance motor performance. Rats were allowed to freely explore the arena for 10 min (habituation phase), then each rat was injected with a saline solution (the same volume as the amphetamine solution) and activity was recorded for 60 min (saline phase). After that, rats received amphetamine doses (0.5 mg/kg) and their activity was assessed for 60 min (amphetamine phase; Figure 3G). We analyzed three variables: (a) total distance walked on the arena (meters), (b)

distance walked in a 10-min period to observe initial motor movements, and (c) average speed per animal per hour.

Immunohistochemistry

Regarding cognitive performance on the third week, a group of animals were deeply anaesthetized with ketamine/xilazine. Subsequently they were perfused with a saline (0.9% NaCl) and heparine (200 μ L/L) solution for 5 min through the left cardiac ventricle, then with 300 mL of 4% paraformaldehyde (PFA, Biopack, Argentina) in 0.1 M phosphate buffer (pH 7.4) for

25 min. Brains were removed, then fixed in the same PFA solution overnight, and stored in 30% sucrose solution (Biopack, Argentina) at 4°C. Coronal sections of the brain, 40 µm thick, were obtained using a freezing microtome (Leica CM15105; Leica Microsystems, Wetzlar, Germany) and collected in phosphate-buffered saline (PBS) 0.01 M in six sets of sections for each animal. For each brain block, one every six serial sections was selected in order to obtain a set of noncontiguous serial sections spanning the whole studied area (CPu, substantia nigra, prefrontal cortex [PFC], and hippocampus). Four animals per group (SHAM and 6-OHDA) were employed ($N=4$ means four set of slices from four different animals). For each animal, three sets of the whole brain sections were used to evaluate reactive TH, ALDH2, and GFAP cells, respectively, in free floating sections under moderate shaking. Three 10-min washes were done in 0.01 M PBS buffer (pH 7.4). Then, the sections were incubated for 1 hr at room temperature in a 10% hydrogen peroxide in 10% methanol solution to quench the endogenous peroxidase activity. After three washes with 0.01 M PBS buffer, sections were incubated in 10% normal horse serum (NHS, Vetacord Comercial, Córdoba, Argentina) for 2 hr under moderate shaking, to block nonspecific binding sites. Immediately, sections were incubated with (a) a polyclonal anti-TH antibody (diluted 1:500, Millipore Cat# AB152, RRID: AB_390204), for 48 hr at 4°C, (b) mouse monoclonal antibody for GFAP (diluted 1:1000, Sigma-Aldrich Cat# G9269, RRID:AB_477035), marker of reactive and resting astrocytes, and (c) mouse monoclonal antiALDH2 antibody (1:1000, Abcam Cat# ab115198, RRID:AB_10900200). Sections were rinsed in 0.01 M PBS buffer and incubated for 2 hr at room temperature with the corresponding anti-rabbit biotinylated secondary antibody (diluted 1:500, Thermo Fisher Scientific Cat# 31820, RRID:AB_228340). Then, after three washes in buffer, they were incubated for 120 min at room temperature with avidin-biotin peroxidase complex (ABC Complex, Vector Laboratories, CA, USA, diluted 1:200). For the immunostaining reaction, we incubated the section with diaminobenzidine (Sigma-Aldrich) in 0.1 M phosphate buffer. Finally, sections were mounted on gelatinized slides, air-dried overnight, dehydrated, cleared in xylene, and coverslipped with DPX mountant for histology (Sigma-Aldrich).

Image Processing

All images were obtained employing a computerized system that includes a Leica DM 4000B microscope equipped with a DFC Leica digital camera attached to a contrast enhancement device. All the images were obtained with identical exposure times, gain and offsets, and saved in TIFF format ($1,392 \times 1,040$ pixels). We

analyzed three different slices from each rat. For PFC, we obtained 6 images, 12 images for CPu, 3 images for dorsal hippocampus, and 3 for SN, from each hemisphere. Right and left hemispheres from each slice had similar results and we averaged data per animal. These brain areas were identified and delimited according to Paxinos and Watson atlas (Paxinos and Watson, 2004). The image analysis was accomplished using IMAGE J software from the National Institute of Health (NIH; <http://rsbweb.nih.gov/ij/>).

Dopamine Cells Reactivity by TH Immunostaining. The analysis of TH+ cells was performed according to the reports by Lindgren et al. (2014). TH-positive fiber density was measured in CPu, PFC, and CA1 using percentage of reactive area with the assessments performed at three equidistant rostrocaudal levels (four photographs per level), spanning from the rostral pole of the striatum (AP: +2.20) to the rostral pole of the globus pallidus (AP: -0.92). Stained sections were taken at $400 \times$ magnification and the area occupied by TH immunostaining was quantified, fixing a threshold of 230 to 215. For SN analyses, we considered number of TH+ cells. For each rat, measurements were taken in both hemispheres in three sections to provide relative data in different experimental conditions but are not intended to be considered as absolute values.

Astrocyte Reactivity by GFAP Immunostaining. GFAP-stained sections were taken at $400 \times$ magnification, and the area occupied by astrocytes was quantified, fixing a threshold of 215 to 170 (depending on the brain area), and expressed as a percentage of the total evaluated area.

Mitochondrial Reactivity by ALDH2 Immunostaining. ALDH2-stained sections were taken at $200 \times$ magnification and ALDH2 mitochondrial reactivity area was quantified, fixing a threshold of 170-230 (depending on the brain area), and expressed as a percentage of the total evaluated area.

Electrophysiology

Rats were sacrificed by guillotine decapitation between 10:00 and 11:00 a.m., to prevent circadian rhythms variations or nonspecific stressors (Teyler and Discenna, 1987). Electrophysiological experiments were carried out using the *in vitro* HP slice preparation (Perez et al., 2010). The hippocampal formation was dissected and transverse slices approximately 400-µm thick were maintained in a storage chamber containing standard Krebs solution (NaCl, 124.3 mM; KCl, 4.9 mM; MgSO₄·7H₂O, 1.3 mM; H₂KPO₄, 1.25 mM; HNaCO₃, 25.6 mM; glucose, 10.4 mM; CaCl₂·2H₂O, 2.3 mM; Sigma, Argentina) saturated with 95% O₂ and 5% CO₂. At the beginning of the experiments, a single slice was placed in a recording

chamber (BSC-BU Harvard Apparatus) perfused with the standard Krebs solution saturated with 95% O₂ and 5% CO₂. The perfusion rate was 1.6 mL/min, and the bathing solution temperature was kept at 28°C with a Temperature Controller (TC-202A Harvard Apparatus). Field excitatory postsynaptic potentials (EPSP) were evoked by an A310 accupulser pulse generator (World Precision Instruments Inc.) with a stimulating electrode made of two twisted wires, which were insulated except for the cut ends (50 µm diameter), which was placed in the perforant path (PP). Then, a recording microelectrode was inserted in the dentate granule cell body layer (Figure 8A). Only slices showing a stable response were included in the study. Amplitude (mV) of EPSP that responded to 0.2 Hz stimuli were sampled for 40 min until EPSP stabilization (baseline; Figure 8B). Once no further changes were observed in the amplitude of EPSP, one of two stimulation protocols was applied. Both protocols were tested in each animal using different slices. In the first protocol (high-frequency stimulation, HFS) LTP was generated using the classical tetanization model consisting of three 100-Hz high-frequency stimulation trains (of 1 s duration each) given at 20 s intervals. In the second protocol applied, the stimulation allowed us to assay different stimulating frequency values in order to determine the minimum value to generate LTP (we called this value *threshold*). The stimulus consisted in a train of square pulses 2 s long, with each square pulse lasting 0.5 ms. We used a stimulus frequency ranging from 10 to 200 Hz. For both protocols, LTP was considered to have occurred when the EPSP amplitude recorded after the stimulus had risen at least 30% from baseline and persisted for 60 min. Once LTP was generated, the EPSP amplitude was recorded every 20 min to register LTP temporal profile (maintenance and magnitude after stimulation protocol). If LTP was not observed 20 min after a given stimulation frequency, another hippocampal slice was used to test a stimulus at the next frequency value.

Statistical Analyses

Statistical analyses were performed using the GraphPad Prism software 6.0 version for Windows (GraphPad Software, Inc, San Diego, CA, USA). Comparisons between groups in different time stages were assessed using analysis of variance (ANOVA) and two-way analyses for repeated measures (RM-ANOVA), Kruskal–Wallis nonparametric test was used for hot plate test. When the ANOVA was significant, Bonferroni was chosen as a post hoc test. Comparisons between groups at a specific time stage were analyzed using Student's *t* test. The LTP results were expressed as percentage of EPSP amplitude change related to the baseline ± standard error of the mean (SEM) and analyzed by repeated two-way measures and the post hoc Holm–Sidak's

multiple comparisons test was employed. Differences were considered statistically significant at $p < .05$.

Results

Three Weeks of 6-OHDA Neurotoxicity Causes Working Memory and Spatial Short-Term Memory Impairments

Y-Maze test was our starting point to settle the period of time in which we would observe cognitive deficits in absence of motor dysfunction. Supplemental Figures A and B summarize the effect of 6-OHDA on working memory throughout 4 weeks. We observed no significant differences at first and second weeks of neurotoxicity on the number of arm entries in Y-Maze apparatus, indicating no motor perturbation— $F(3, 83) = 0.93$; $p = .43$. At fourth week, half of the animals of 6-OHDA group were excluded by test selection criteria, suggesting motor alteration (black arrow; Supplemental Figure A). Supplemental Figure B shows the percentage of alternation performed by each experimental group— $F(3, 83) = 0.96$; $p = .41$. With this last result, we focused on third week since statistical analyses revealed significant differences in this stage. Both groups made similar number of arm entries ($t = 0.89$; $p = .38$, Figure 2B), but there were significant changes in the percentage of alternations between SHAM and 6-OHDA rats ($t = 2.83$; $p = .008$, Figure 2C). Taken together, these results suggest that cognitive deficits at 3 weeks of neurotoxicity are not correlated with motor alterations.

Based on these results, we further investigated whether 6-OHDA causes short term memory impairments. Modified Y-Maze showed that in the training session, both groups made similar percentages of arm entries— $F(1, 24) = 0.004$; $p = .95$, Figure 2E—and explored similar times during both trial sessions of the test— $F(1, 24) = 0.127$; $p = .72$, Figure 2F—indicating no motor dysfunctions. Statistical analyses indicated no significant differences between the interaction of treatment and arm explored— $F(2, 36) = 3.13$; $p = .055$, Figure 2G. However, when we only compared the exploration in the novel arm (Arm 3), 6-OHDA rats had a lower percentage of entries with respect to SHAM rats ($t = 2.81$; $p = .0158$, Figure 2H). Regarding the difference of exploration between the new and the old location, the group treated with 6-OHDA had an impaired short-term memory ($t = 4.9$; $p < .0012$, Figure 2J).

6-OHDA Treatment Does Not Affect Motor Performance Over the First Three Weeks of Neurodegeneration

In motor analysis, there were no significant differences in latency times evaluated in the horizontal wire mesh pole task ($t = 0.77$; $p = .44$, Figure 3B). In Supplemental

Figure C, we analyzed the interaction for the treatment and time interaction throughout the 4 weeks of neurotoxicity— $F(3, 60)=1.14$; $p=.34$. However, multiple t tests post hoc show that after 4 weeks of neurodegeneration there is a significant reduction of latency time in 6-OHDA group compared to the SHAM group ($p=.027$).

In addition, we evaluated sensitivity and motor performance with a thermal nociception exposure. At third week, no statistical differences were observed in initial time of nociception ($U=118$; $p=.38$, Figure 3D), final time to escape of stimulus ($U=118$; $p=.37$, Figure 3E) and reaction time ($U=122$; $p=.44$, Figure 3F). We observed hot plate performance in each neurodegenerative stage and we found significant differences when we analyzed the same treatment among stages for initial times ($H_7=41.49$, Supplemental Figure D). During the first week of neurotoxicity, 6-OHDA group showed an increased level of nociception compared with its corresponding counterpart at the 3rd week ($p<.01$), the same difference was observed in the SHAM group ($p<.0001$; Supplemental Figure D). There were no significant differences regarding times taken to escape from stimulus ($H_7=13.51$; $p=.06$, Supplemental Figure E). Furthermore, the reaction times were similar for both experimental groups in the four stages ($H_7=7.89$; $p=.34$, Supplemental Figure F).

To exclude that cognitive deficits observed in 6-OHDA rats are independent of motor deficits, we performed a locomotor activity task induced by amphetamine administration at third week of neurotoxicity. Both experimental groups walked similar distances after amphetamine administration— $F(1, 32)=0.28$; $p=.6$ (see Figure 3H). However, there was a significant difference between drugs (Saline vs. Amphetamine) in both groups ($p<.0001$). We also analyzed distance travelled per minute and average speed, and both groups had similar performances, indicating absence of initiation movement disturbances— $F(5, 20)=0.24$; $p=.93$ (see Figure 3I)—and covered similar distances in the same time ($t=0.92$; $p=.36$, Figure 3J). Taking cognitive results and strength performance regarding the fourth week, we observed a significant reduction of distance travelled by 6-OHDA rats after amphetamine administration ($p=.02$, Supplemental Figure G). According to this, bilateral intradorsolateral 6-OHDA injection in the CPU was sufficient to cause cognitive impairments without motor alterations at 3 weeks postlesion.

6-OHDA Causes Changes in Dopaminergic Neurons, Astrocytes, and Mitochondrial Immunoreactivity in the Brain Areas Involved

Prefrontal Cortex. Intradorsolateral CPU administration of 6-OHDA (20 μ g per hemisphere) caused significant

differences between groups on the staining of TH and ALDH2 enzyme after 21 days of neurotoxicity. There were no significant differences between both hemispheres, so we calculated the average of both sides for each treatment. Student t test analysis revealed a significant effect of 6-OHDA in the percentage of TH positive area ($t=2.61$; $p=.045$, Figure 4A). Figure 4B and C shows representative examples of TH immunoreactivity in SHAM and 6-OHDA groups, respectively. No significant differences were observed in astrocytes reactivity ($t=0.057$; $p=.95$, Figure 4D). Figure 4E and F shows representative examples of GFAP immunoreactivity in SHAM and 6-OHDA groups, respectively. Furthermore, we found a significant decrease in ALDH2 expression in 6-OHDA group ($t=3.51$; $p=.017$, Figure 4G). Figure 4H and I is representative examples of ALDH2 immunoreactivity in SHAM and 6-OHDA groups, respectively.

Hippocampus. Statistical analyses revealed no significant effect of 6-OHDA in the amount of percentage of TH positive area ($t=0.593$; $p=.95$, Figure 5A). Figure 5B and C shows representative examples of TH immunoreactivity in SHAM and 6-OHDA groups, respectively. Significant differences were observed in astrocytes reactivity ($t=2.55$; $p=.04$, Figure 5D). Figure 5E and F shows representative examples of GFAP immunoreactivity in SHAM and 6-OHDA groups, respectively. Furthermore, we found a significant decrease in ALDH2 expression in 6-OHDA group ($t=5.01$; $p=.0025$, Figure 5G). Figure 5H and I is representative examples of ALDH2 immunoreactivity in SHAM and 6-OHDA groups, respectively.

Cpu. 6-OHDA induced a decrease in the percentages of TH positive area, respect to the SHAM group ($t=10.76$; $p=.0001$, Figure 6A). Figure 6B and C shows representative examples of TH immunoreactivity in SHAM and 6-OHDA groups, respectively. Significant differences were observed in astrocytes reactivity ($t=5.40$; $p=.0031$, Figure 6D). Figure 6E and F shows representative examples of GFAP immunoreactivity in SHAM and 6-OHDA groups, respectively. Moreover, ALDH2 immunoreactivity was decreased in 6-OHDA group ($t=6.15$; $p=.0082$, Figure 6G). Figure 6H and I is representative examples of ALDH2 immunoreactivity in SHAM and 6-OHDA groups, respectively.

Substantia Nigra. After 3 weeks of neurotoxicity, 6-OHDA caused a significant reduction in the number of TH positive cells, respect to the SHAM group ($t=3.09$; $p=.0392$, Figure 7A). Figure 7B and C shows representative examples of TH immunoreactivity in SHAM and 6-OHDA groups, respectively. No significant differences were observed in astrocytes reactivity ($t=0.236$; $p=.82$, Figure 7D). Figure 7E and F shows representative

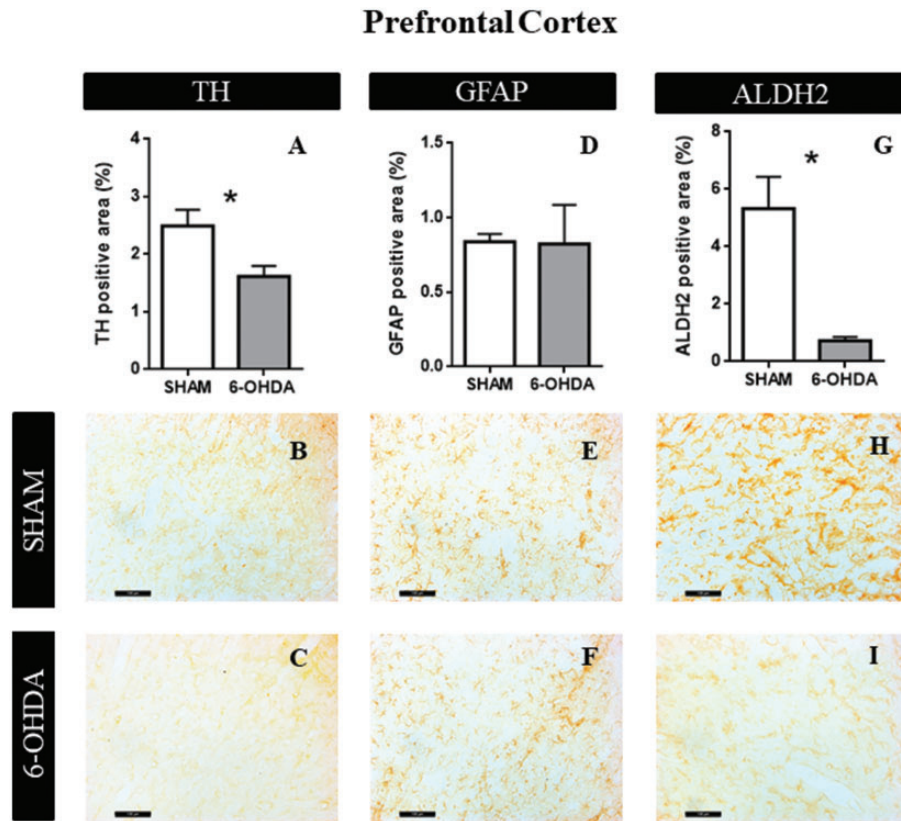


Figure 4. Structural Characteristics in PFC. A: The graphs show TH positive area ($n=4$). B: Representative images at $20\times$ magnification of SHAM group. C: Representative images at $20\times$ magnification of 6-OHDA group. D: GFAP positive area quantification ($n=4$). E: Representative images at $20\times$ magnification of SHAM group. F: Representative images at $20\times$ magnification of 6-OHDA group. G: ALDH2 percentage of positive area ($n=4$). Values are the mean \pm SEM for the experimental groups. * $p < .05$; black bar scale = $100\ \mu\text{m}$. TH = tyrosine hydroxylase; GFAP = glial fibrillar acid protein; ALDH2 = aldehyde dehydrogenase 2.

examples of GFAP immunoreactivity in SHAM and 6-OHDA groups, respectively. As well as TH expression, ALDH2 immunoreactivity was reduced in 6-OHDA group ($t=2.91$; $p=.033$, Figure 7G). Figure 7H and I shows representative examples of ALDH2 immunoreactivity in SHAM and 6-OHDA groups, respectively.

6-OHDA Causes LTP Impairments in Hippocampus

In this study, we observed that in the 6-OHDA group the LTP was not generated using the threshold protocol, while in the SHAM group LTP was generated at 100 Hz. In Figure 8A and B, we can observe a hippocampal slice sketch indicating the position of the stimulating and recording electrodes and how measurements of EPSP are taken by EPSP sample traces (Figure 8A and B, respectively). The two-way ANOVA analysis showed a significant effect of Treatment \times Threshold interaction— $F(3, 21)=8.67$; $p=.0006$, Figure 8C. Holm–Sidak’s multiple comparisons test showed a significant increase in the % EPSP in the SHAM group ($43.4 \pm 10.6\%$) at 100 Hz when compared to 6-OHDA group ($-2.7 \pm 8.8\%$; $p < .05$). Within the SHAM group the % EPSP at 100Hz was

significantly different from 40 ($-6.4 \pm 6.8\%$), 60 ($-1.5 \pm 4.2\%$), and 80 Hz ($8.1 \pm 3.4\%$; $p < .05$). In the 6-OHDA group, no differences were found in the % EPSP at any frequency ($p > .05$). In contrast, when the temporal profile of LTP maintenance after HFS protocol was analyzed, LTP was generated in both groups. The repeated measures two-way ANOVA showed a significant effect of time— $F(5, 35)=22.74$; $p=.0001$ —without effect of group \times time interaction— $F(5, 35)=0.38$; $p=.86$, Figure 8D. Holm–Sidak’s multiple comparisons test also showed significant differences in the % of increase respect to EPSP baseline between times before *tetanus* (-40 and -20 min) and times after *tetanus* (0, 20, 40, and 60 min, $p < .05$). No differences were observed in 0, 20, 40, and 60 min between groups ($p > .05$, Figure 8E).

Discussion

Currently, memory deficit symptoms are increasingly recognized in neurodegenerative diseases, even at early disease stages as a result of hippocampal malfunctioning (Christopher et al., 2014; Aarsland, 2015). In this study, we showed an early working and spatial memory

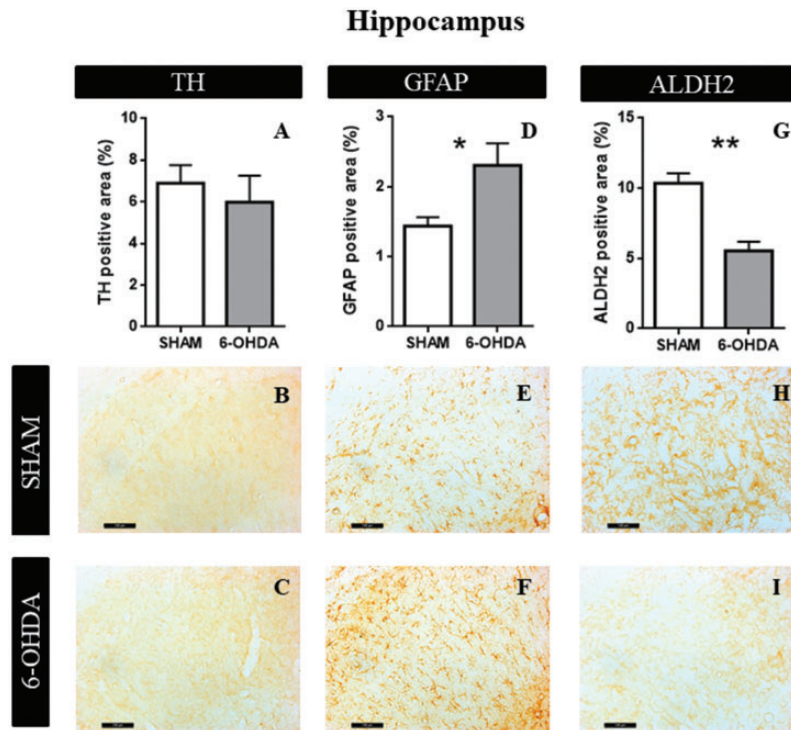


Figure 5. Structural characteristics in hippocampus (CA1). A: The graphs show TH positive area ($n = 4$). B: Representative images at $20\times$ magnification of SHAM group. C: Representative images at $20\times$ magnification of 6-OHDA group. D: GFAP positive area quantification ($n = 4$). E: Representative images at $20\times$ magnification of SHAM group. F: Representative images at $20\times$ magnification of 6-OHDA group. G: ALDH2 percentage of positive area ($n = 4$). Values are the mean \pm SEM for the experimental groups. * $p < .05$. ** $p < .01$; black bar scale = $100\ \mu\text{m}$. TH = tyrosine hydroxylase; GFAP = glial fibrillar acid protein; ALDH2 = aldehyde dehydrogenase 2.

impairment prior to motor dysfunctions in a Parkinsonism neurotoxicity animal model, suggesting that mechanisms linked to the nigrostriatal pathway may modulate hippocampal cognitive processes with ALDH2 and astrocyte participation.

Early Cognitive Impairments Before Motor Dysfunction

Failure of different neurotransmitter circuits may be involved in the dysfunction of synaptic plasticity modulation between striatum, prefrontal cortex, and hippocampus, leading to different NMS (Williams-Gray et al., 2009; Kehagia et al., 2010). Several arguments support the choice of a bilateral model instead of the more widely used unilateral lesion model (Deumens et al., 2002; Orth and Tabrizi, 2003). In this study, using an appropriate dose of the neurotoxin, we successfully handled the remarkable aphagia and adipsia, as consequence of dopaminergic system imbalances that negatively impact on body weight and in the survival rate of animals reported in previous analysis.

Regarding this model, different learning and memory deficits were characterized using a variety of behavioral tasks such as object recognition (Bonito-Oliva et al., 2014), social recognition (Tadaiesky et al., 2008), Morris water maze (Tadaiesky et al., 2008; Braun et al.,

2012), and Y-maze (Pioli et al., 2008; Matheus et al., 2016). In this context, it is important to highlight that a good motor performance is required to support an appropriate cognitive function evaluation. Matheus et al. (2016) found short term memory deficit at third week using a modified Y-Maze and novel object recognition after neurotoxic administration. Our data are consistent with the fact that short term cognitive deficit appears at third week. Moreover, and considering that several of the initial cognitive deficits are described as a failure in the cognitive corticostriatal loop (ventrolateral prefrontal cortex, caudate nucleus, and thalamus), involving executive defects in planning, initiation and visuospatial memory (Pagonabarraga and Kulisevsky, 2012), we decided to evaluate Y maze working memory task, since it could be indicative of a failure in this loop. We also found short-term memory dysfunctions through the assessments of modified Y-Maze and NLR. In the abovementioned paper, Matheus et al. found motor dysfunction 21 days after injection (by OF, rotarod, and grip force tests). However, in our experimental conditions, we observed motor alteration 4 weeks after 6-OHDA administration (by locomotor activity task induced by amphetamine administration at third and fourth weeks of neurotoxicity). Our results showed the dysfunction of

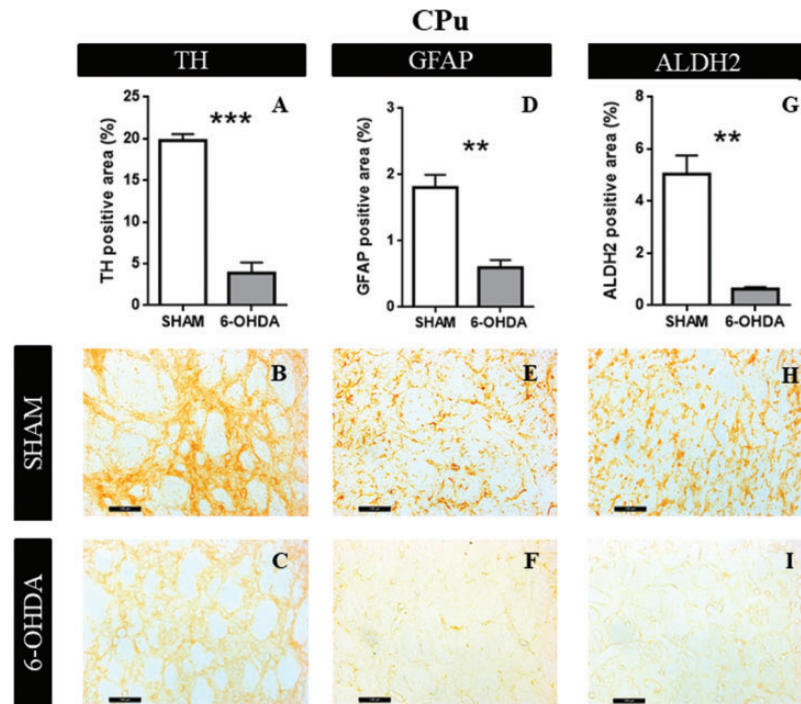


Figure 6. Structural characteristics in Caudate Putamen Unit. A: The graphs show TH positive area ($n = 4$). B: Representative images at $20\times$ magnification of SHAM group. C: Representative images at $20\times$ magnification of 6-OHDA group. D: GFAP positive area quantification ($n = 4$). E: Representative images at $20\times$ magnification of SHAM group. F: Representative images at $20\times$ magnification of 6-OHDA group. G: ALDH2 percentage of positive area ($n = 4$). Values are the mean \pm SEM for the experimental groups. * $p < .05$; ** $p < .01$; *** $p < .0001$ black bar scale = 100 μm . TH = tyrosine hydroxylase; GFAP = glial fibrillar acid protein; ALDH2 = aldehyde dehydrogenase 2; CPu = caudate putamen unit.

both working and spatial cognitive processes, suggesting that the hippocampus could be effectively affected by 6 OHDA neurotoxicity effects.

According to Holdstock et al. (2000), declarative spatial memory can be subdivided into allocentric spatial memory (memory of the position of objects or stimuli, which is independent of the observer) and egocentric spatial memory (which is related to the observer). Specifically, the hippocampus is involved through the allocentric and dorsolateral striatum in the egocentric spatial memory (Sarkisyan and Hedlund, 2009). These findings suggest that many aspects of cognitive alterations, after neurotoxin injection, could be involved in the interaction, not only between the striatum and the prefrontal cortex but also the dorsal hippocampal circuit (Cropley et al., 2006; Moustafa et al., 2008; Miah et al., 2012). Despite the fact that CPu area receives the main impact of the neurotoxin and leads to decreased astrocytic positive area, other brain regions are involved. In this study, we observed mitochondrial ALDH2 enzyme changes in four brain areas namely, the CPu, SNpc, PFC, and hippocampus. Regarding this, we found lower ALDH2 enzyme expression, suggesting that in CPu, 6-OHDA neurotoxicity triggers the production of ROS and probably brain mitochondrial dysfunction.

Consequently, it has been reported that ROS production due to 6-OHDA auto-oxidation leads to mitochondrial homeostasis failure and the induction of apoptosis via an increase in caspases3/7 and PCKdelta expressions *in vitro* (Hanrott et al., 2006).

Aldehyde dehydrogenase 2 (ALDH2) plays a crucial role in maintaining a proper metabolism by detoxifying cells from aldehydic substrates (Chen et al., 2016). In PD dopaminergic circuits, DOPAL and 4-HNE accumulation leads to protein-adduct formation and neurotoxicity by inactivation of ALDH2 (Florang et al., 2007). These alterations were attenuated by Alda-1 administration, a potent activator of ALDH2 (Chiu et al., 2015).

Thus, our results are in concordance with the idea that in our experimental model, reactive aldehyde accumulation may inhibit ALDH2 and trigger mitochondrial dysfunction leading to a higher aldehyde-induced damage in several brain areas (Goldstein et al., 2013).

As we mentioned earlier, this cognitive decline is expressed in absence of motor alterations, showing that the system still maintains the motor function despite the loss of dopaminergic neurons. In this aspect, an important compensatory role could be led by (a) the presence of others neurotransmitters involved in the presynaptic release of dopamine such as serotonin, acetylcholine,

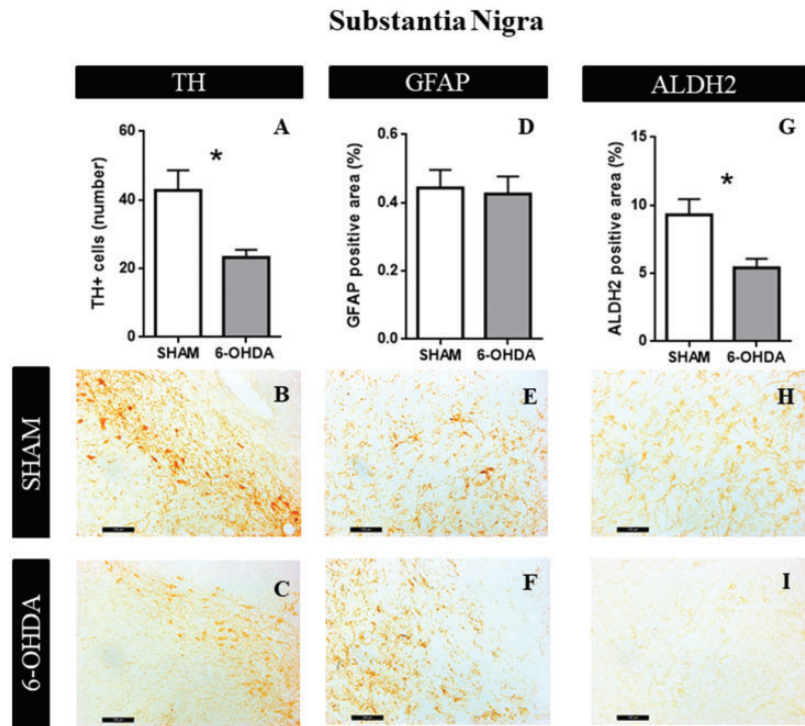


Figure 7. Structural Characteristics in Substantia Nigra. A: The graphs show TH positive area ($n = 4$). B: Representative images at $20\times$ magnification of SHAM group. C: Representative images at $20\times$ magnification of 6-OHDA group. D: GFAP positive area quantification ($n = 4$). E: Representative images at $20\times$ magnification of SHAM group. F: Representative images at $20\times$ magnification of 6-OHDA group. G: ALDH2 percentage of positive area ($n = 4$). Values are the mean \pm SEM for the experimental groups. * $p < .05$; black bar scale = $100\ \mu\text{m}$. TH = tyrosine hydroxylase; GFAP = glial fibrillar acid protein; ALDH2 = aldehyde dehydrogenase 2.

glutamate, and GABA (Casas et al., 2013; Pfeiffer et al., 2014); (b) the hyperfunction of postsynaptic DA receptors, and (c) the alteration of dopaminergic afferents (Calabresi et al., 2013). Moreover, morphological modifications in type and sizes of medium spiny neurons spines (Villalba and Smith, 2017); plastic synaptic changes (Schirinzi et al., 2016) and enhanced DA synthesis by alternative biochemical pathways (Kozina et al., 2017) could be implicated. Besides, partial lesions in the caudate-putamen complex lead to a selective and gradual depletion of the nigrostriatal dopaminergic system (Deumens et al., 2002). A dorsal-ventral distinction of the striatum was characterized as well as a mediolateral-oriented functional striatal gradient, where the dorsolateral striatal area is more implicated in cognitive processes (Voorn et al., 2004).

Hypofunction of Hippocampal Circuits

Cognitive impairment is proposed to involve a hypofunction of frontocortico-striatal circuits (Christopher et al., 2014). Moreover, the loss of nigrostriatal dopaminergic neurons affects different mesolimbic structures such as the hippocampus, which, as previously mentioned, is critically involved in plastic processes underlying learning and memory. In fact, according to our results, the specific

hippocampal increases of GFAP reactive area probably suggest astrocyte participation, to contribute to restoring the cognitive dysfunction involved. Spatial learning and memory functions are affected by dopaminergic alterations, in particular hippocampal LTP (Bonito-Oliva et al., 2014). Our study confirms these previous observations, respecting hippocampus may play an important role in the pathophysiology of this neurodegenerative framework. A synaptic transmission dysfunction was observed as an impaired response in dentate gyrus to a weak stimulation (threshold protocol) able to induce LTP in the SHAM group. This impairment was no longer observed when a stronger stimuli (HFS protocol) was applied, indicating that hippocampal plasticity can be induced at a higher stimulation levels. Our results are consistent with those observed in PFC circuit by Matheus et al. (2016), suggesting that hippocampal dysfunction accompanies the defective synaptic plasticity through dopaminergic circuits that modulate hippocampal activity. These set of finding points to the DG as a critical structure involved in the memory deficit produced by partial DA depletion. The understanding of this neurodegenerative progression may pave the way for the development of novel therapeutic strategies focused on the observed cognitive dysfunction. In addition to the

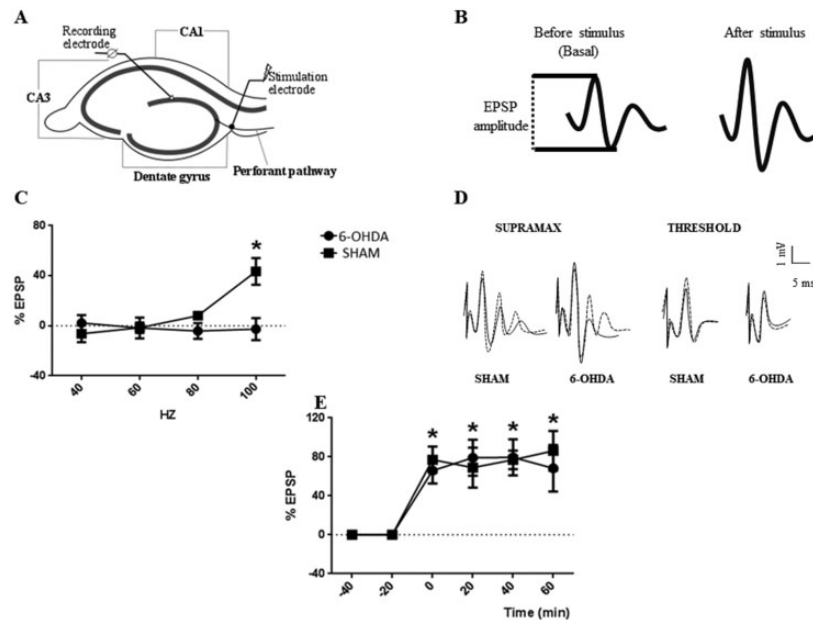


Figure 8. Long-Term Potentiation Analysis Following 6-OHDA Administration. A: Hippocampal slice cartoon indicating the position of the stimulating and recording electrodes. B: EPSP sample traces show how measurements of EPSP are taken. C: Graph show increments in EPSP, as percentage of basal EPSP after different frequency stimulation (threshold protocol) for 6-OHDA and SHAM groups, $*p < .05$ compared to all frequency stimulation (Hz) in both groups. D: EPSP sample traces for 6-OHDA and SHAM groups before (full line) and after (dotted line) effective stimulation. E: Time course graph show increments in EPSP, as % of basal EPSP, after HFS protocol in 6-OHDA and SHAM groups, $*p < .05$ compared to basal (-40 and -20 min) in both groups. ($n = 4$). For (C) and (D) symbols, values are the mean \pm SEM. EPSP = excitatory postsynaptic potentials.

known cognitive alteration, our work is the first that explores a possible participation of ALDH2 and astrocytes into CPu-SNpc-PFC-Hippocampal circuit affected in nigrostriatal injured animals with hippocampal cognitive dysfunctions.

Summing up, this study shows that our experimental paradigm is associated with the hippocampus, suggesting that cognitive impairment could be related to a deficit in the nigrostriatal-cortical-hippocampal-circuit. We postulate that our 6-hydroxydopamine animal model is able to trigger cognitive impairment before appearance of motor symptoms, which makes the model suitable to follow the response to treatment. Our data prompt us to conduct further studies using this experimental model that should allow the exploration of new therapies focused on hippocampal dysfunction.

Summary

- Selective bilateral lesions of the dopaminergic system in dorsal CPu, lead to working and spatial memory impairments after three weeks of 6-OHDA induced neurotoxicity.
- A bilateral depletion of the nigrostriatal circuit is associated with impairment in long-term potentiation (LTP) generation in the hippocampus dentate gyrus,

suggesting that this treatment affects hippocampal synaptic transmission.

- Astrocytes and mitochondrial ALDH2 enzyme are associated with to brain specific altered properties that negatively affect hippocampal function on the 3rd week after 6-OHDA toxicity.

Acknowledgments

The authors thank Estela Salde, Lorena Mercado and Leandro Oliveros for technical assistance, Yanina Altamirano and Javier Reparaz for animal care, Dr. Rodolfo Goya for his theoretical and redaction assistance, and Ms. Irene McCarthy for language and redaction revision.

Author Contributions

M. L. H. did behavioral studies and data analysis. M. S. G. and E. A. V. performed the LTP protocols. M. L. H. and R. D. P. did the TH, GFAP, and ALDH2 immunostaining, performed the analysis, interpretation, and designed the different plots and graphs. M. L. H., M. B. V., C. B. H., M. J. B., and M. F. P. wrote different sections of the manuscript. M. L. H., V. A. M., C. B. H., and M. J. B. assembled the final version of the paper.

Declaration of Conflicting Interests

The author(s) declared no potential conflicts of interest with respect to the research, authorship, and/or publication of this article.

Funding

The author(s) disclosed receipt of the following financial support for the research, authorship, and/or publication of this article: This study was supported by grants from PICT Grant to Maria Jose Bellini-Préstamo BID (2013-1119) and Universidad Nacional de La Plata Grant M184 to Claudia Hereñú (2015–2018). Ethical Approval all procedures were handled in accordance with the NIH Guide for the Care and Use of Laboratory Animals as approved by the Animal Care and Use Committee of the Facultad de Ciencias Químicas, Universidad Nacional de Córdoba, Argentina (0030162/2017).

ORCID iD

Claudia B. Hereñú  <https://orcid.org/0000-0002-3135-7024>

Supplemental material

Supplemental material for this article is available online.

References

- Aarsland, D. (2015). Cognitive impairment in Parkinson's disease and dementia with Lewy bodies. *Parkinsonism & Related Disorders*, 22(Suppl 1), S144–S148. <https://doi.org/10.1016/j.parkreldis.2015.09.034>
- Aarsland, D., Creese, B., Politis, M., Chaudhuri, K. R., ffytche, D. H., Weintraub, D., & Ballard, C. (2017). Cognitive decline in Parkinson disease. *Nature Reviews Neurology*, 13(4), 217–231. <https://doi.org/10.1038/nrneuro.2017.27>
- Aarsland, D., & Kurz, M. W. (2010). The epidemiology of dementia associated with Parkinson's disease. *Brain Pathology*, 20(3), 633–639. <https://doi.org/10.1111/j.1750-3639.2009.00369.x>
- Allen, N. J. (2014). Astrocyte regulation of synaptic behavior. *Annual Review of Cell and Developmental Biology*, 30(1), 439–463. <https://doi.org/10.1146/annurev-cellbio-100913-013053>
- Bazzari, A. H., & Parri, H. R. (2019). Neuromodulators and long-term synaptic plasticity in learning and memory: A steered-glutamatergic perspective. *Brain Sciences*, 9(11), 300. <https://doi.org/10.3390/brainsci9110300>
- Björklund, A., & Dunnett, S. B. (2019). The amphetamine induced rotation test: A re-assessment of its use as a tool to monitor motor impairment and functional recovery in rodent models of Parkinson's disease. *Journal of Parkinson's Disease*, 9(1), 17–29. <https://doi.org/10.3233/JPD-181525>
- Boix, J., Padel, T., & Paul, G. (2015). A partial lesion model of Parkinson's disease in mice—Characterization of a 6-OHDA-induced medial forebrain bundle lesion. *Behavioural Brain Research*, 284, 196–206. <https://doi.org/10.1016/j.bbr.2015.01.053>
- Bonito-Oliva, A., Pignatelli, M., Spigolon, G., Yoshitake, T., Seiler, S., Longo, F., Piccinin, S., Kehr, J., Mercuri, N. B., Nistico, R., & Fisone, G. (2014). Cognitive impairment and dentate gyrus synaptic dysfunction in experimental Parkinsonism. *Biological Psychiatry*, 75(9), 701–710. <https://doi.org/10.1016/j.biopsych.2013.02.015>
- Braak, H., Rüb, U., Gai, W. P., & Del Tredici, K. (2003). Idiopathic Parkinson's disease: Possible routes by which vulnerable neuronal types may be subject to neuroinvasion by an unknown pathogen. *Journal of Neural Transmission*, 110(5), 517–536. <https://doi.org/10.1007/s00702-002-0808-2>
- Braun, A. A., Graham, D. L., Schaefer, T. L., Skelton, M. R., Williams, M. T., & Vorhees, C. V. (2012). Dorsal striatal dopamine depletion impairs both allocentric and egocentric navigation in rats. *Neurobiology of Learning and Memory*, 97(4), 402–408. <https://doi.org/10.1016/j.nlm.2012.03.004>
- Broussard, J. I., Yang, K., Levine, A. T., Tsetsenis, T., Jenson, D., Cao, F., Garcia, I., Arenkiel, B. R., Zhou, F. M., De Biasi, M., & Dani, J. A. (2016). Dopamine regulates aversive contextual learning and associated in vivo synaptic plasticity in the hippocampus. *Cell Reports*, 14(8), 1930–1939. <https://doi.org/10.1016/j.celrep.2016.01.070>
- Calabresi, P., Castrioto, A., Di Filippo, M., & Picconi, B. (2013). New experimental and clinical links between the hippocampus and the dopaminergic system in Parkinson's disease. *The Lancet Neurology*, 12(8), 811–821. [https://doi.org/10.1016/S1474-4422\(13\)70118-2](https://doi.org/10.1016/S1474-4422(13)70118-2)
- Casas, S., Giuliani, F., Cremaschi, F., Yunes, R., & Cabrera, R. (2013). Neuromodulatory effect of progesterone on the dopaminergic, glutamatergic, and GABAergic activities in a male rat model of Parkinson's disease. *Neurological Research*, 35(7), 719–725. <https://doi.org/10.1179/1743132812Y.0000000142>
- Chen, C. H., Joshi, A. U., & Mochly-Rosen, D. (2016). The role of mitochondrial aldehyde dehydrogenase 2 (ALDH2) in neuropathology and neurodegeneration. *Acta Neurologica Taiwanica*, 25(4), 111–123. <https://doi.org/10.1038/srep30424>
- Chiu, C. C., Yeh, T. H., Lai, S. C., Wu-Chou, Y. H., Chen, C. H., Mochly-Rosen, D., Huang, Y. C., Chen, Y. J., Chen, C. L., Chang, Y. M., Wang, H. L., & Lu, C. S. (2015). Neuroprotective effects of aldehyde dehydrogenase 2 activation in rotenone-induced cellular and animal models of Parkinsonism. *Experimental Neurology*, 263, 244–253. <https://doi.org/10.1016/j.expneurol.2014.09.016>
- Christopher, L., Marras, C., Duff-Canning, S., Koshimori, Y., Chen, R., Boileau, I., Segura, B., Monchi, O., Lang, A. E., Rusjan, P., Houle, S., & Strafella, A. P. (2014). Combined insular and striatal dopamine dysfunction are associated with executive deficits in Parkinson's disease with mild cognitive impairment. *Brain*, 137(2), 565–575. <https://doi.org/10.1093/brain/awt337>
- Commins, D. L., Shaughnessy, R. A., Axt, K. J., Vosmer, G., & Seiden, L. S. (1989). Variability among brain regions in the specificity of 6-hydroxydopamine (6-OHDA)-induced lesions. *Journal of Neural Transmission*, 77(2–3), 197–210. <https://doi.org/10.1007/BF01248932>
- Crispim Junior, C. F., Pederiva, C. N., Bose, R. C., Garcia, V. A., Lino de Oliveira, C., & Marino Neto, J. (2012). ETHOWATCHER: Validation of a tool for behavioral and video-tracking analysis in laboratory animals. *Computers in Biology and Medicine*, 42(2), 257–264. <https://doi.org/10.1016/j.combiomed.2011.12.002>
- Cropley, V. L., Fujita, M., Innis, R. B., & Nathan, P. J. (2006). Molecular imaging of the dopaminergic system and its

- association with human cognitive function. *Biological Psychiatry*, 59(10), 898–907. <https://doi.org/10.1016/j.biopsych.2006.03.004>
- Deumens, R., Blokland, A., & Prickaerts, J. (2002). Modeling Parkinson's disease in rats: An evaluation of 6-OHDA lesions of the nigrostriatal pathway. *Experimental Neurology*, 175(2), 303–317. <https://doi.org/10.1006/exnr.2002.7891>
- Deza-Ponzio, R., Herrera, M. L., Bellini, M. J., Virgolini, M. B., & Hereñu, C. B. (2018). Aldehyde dehydrogenase 2 in the spotlight: The link between mitochondria and neurodegeneration. *NeuroToxicology*, 68, 19–24. <https://doi.org/10.1016/j.neuro.2018.06.005>
- Ehgoetz Martens, K. A., & Lewis, S. J. G. (2017). Pathology of behavior in PD: What is known and what is not? *Journal of the Neurological Sciences*, 374, 9–16. <https://doi.org/10.1016/j.jns.2016.12.062>
- Florang, V. R., Rees, J. N., Brogden, N. K., Anderson, D. G., Hurley, T. D., & Doorn, J. A. (2007). Inhibition of the oxidative metabolism of 3,4-dihydroxyphenylacetaldehyde, a reactive intermediate of dopamine metabolism, by 4-hydroxy-2-nonenal. *NeuroToxicology*, 28(1), 76–82. <https://doi.org/10.1016/j.neuro.2006.07.018>
- Goldstein, D. S., Sullivan, P., Holmes, C., Miller, G. W., Alter, S., Strong, R., Mash, D. C., Kopin, I. J., & Sharabi, Y. (2013). Determinants of buildup of the toxic dopamine metabolite DOPAL in Parkinson's disease. *Journal of Neurochemistry*, 126(5), 591–603. <https://doi.org/10.1111/jnc.12345>
- Hanrott, K., Gudmunsen, L., O'Neill, M. J. & Wonnacott, S. (2006). 6-Hydroxydopamine-induced apoptosis is mediated via extracellular auto-oxidation and caspase 3-dependent activation of protein kinase C δ . *Journal of Biological Chemistry*, 281(9), 5373–5382. <https://doi.org/10.1074/jbc.M511560200>
- Herrera, M. L., Falomir-Lockhart, E., Dolcetti, F. J. C., Arnal, N., Bellini, M. J., & Hereñu, C. B. (2019). Implication of Oxidative Stress, Aging, and Inflammatory Processes in Neurodegenerative Diseases: Growth Factors as Therapeutic Approach. In: *Psychiatry and Neuroscience Update*. Cham: Springer International Publishing, pp. 165–176. https://doi.org/10.1007/978-3-319-95360-1_14
- Holdstock, J. S., Mayes, A. R., Cezayirli, E., Isaac, C. L., Aggleton, J. P., & Roberts, N. (2000). A comparison of egocentric and allocentric spatial memory in a patient with selective hippocampal damage. *Neuropsychologia*, 38(4), 410–425. [https://doi.org/10.1016/S0028-3932\(99\)00099-8](https://doi.org/10.1016/S0028-3932(99)00099-8)
- Kehagia, A. A., Barker, R. A., & Robbins, T. W. (2010). Neuropsychological and clinical heterogeneity of cognitive impairment and dementia in patients with Parkinson's disease. *The Lancet Neurology*, 9(12), 1200–1213. [https://doi.org/10.1016/S1474-4422\(10\)70212-X](https://doi.org/10.1016/S1474-4422(10)70212-X)
- Kirik, D., Rosenblad, C., & Björklund, A. (1998). Characterization of behavioral and neurodegenerative changes following partial lesions of the nigrostriatal dopamine system induced by intrastriatal 6-hydroxydopamine in the rat. *Experimental Neurology*, 152(2), 259–277. <https://doi.org/10.1006/exnr.1998.6848>
- Kozina, E. A., Kim, A. R., Kurina, A. Y., & Ugrumov, M. V. (2017). Cooperative synthesis of dopamine by non-dopaminergic neurons as a compensatory mechanism in the striatum of mice with MPTP-induced Parkinsonism. *Neurobiology of Disease*, 98(October), 108–121. <https://doi.org/10.1016/j.nbd.2016.12.005>
- Lindgren, H. S., Demirbugen, M., Bergqvist, F., Lane, E. L., & Dunnett, S. B. (2014). The effect of additional noradrenergic and serotonergic depletion on a lateralised choice reaction time task in rats with nigral 6-OHDA lesions. *Experimental Neurology* 253, 52–62. <https://doi.org/10.1016/j.expneurol.2013.11.015>
- Matheus, F. C., Rial, D., Real, J. I., Lemos, C., Ben, J., Guaita, G. O., Pita, I. R., Sequeira, A. C., Pereira, F. C., Walz, R., Takahashi, R. N., Bertoglio, L. J., Da Cunha, R. A., & Prediger, R. D. (2016). Decreased synaptic plasticity in the medial prefrontal cortex underlies short-term memory deficits in 6-OHDA-lesioned rats. *Behavioural Brain Research*, 301, 43–54. <https://doi.org/10.1016/j.bbr.2015.12.011>
- Miah, I. P., Olde Dubbelink, K. T., Stoffers, D., Deijen, J. B., & Berendse, H. W. (2012). Early-stage cognitive impairment in Parkinson's disease and the influence of dopamine replacement therapy. *European Journal of Neurology*, 19(3), 510–516. <https://doi.org/10.1111/j.1468-1331.2011.03578.x>
- Mokry, J. (1995). *Experimental models and behavioural tests used in the study of Parkinson's disease*. Physiological Research/Academia Scientiarum Bohemoslovaca.
- Moustafa, A. A., Sherman, S. J., & Frank, M. J. (2008). A dopaminergic basis for working memory, learning and attentional shifting in Parkinsonism. *Neuropsychologia*, 46(13), 3144–3156. <https://doi.org/10.1016/j.neuropsychologia.2008.07.011>
- Nishida, F., Morel, G. R., Hereñu, C. B., Schwerdt, J. I., Goya, R. G., & Portiansky, E. L. (2011). Restorative effect of intracerebroventricular insulin-like growth factor-I gene therapy on motor performance in aging rats. *Neuroscience*, 177, 195–206. <https://doi.org/10.1016/j.neuroscience.2011.01.013>
- Occhieppo, V. B., Marchese, N. A., Rodríguez, I. D., Basmadjian, O. M., Baiardi, G., & Bregonzio, C. (2017). Neurovascular unit alteration in somatosensory cortex and enhancement of thermal nociception induced by amphetamine involves central AT1receptor activation. *European Journal of Neuroscience*, 45(12), 1586–1593. <https://doi.org/10.1111/ejn.13594>
- Orth, M., & Tabrizi, S. J. (2003). Models of Parkinson's disease. *Movement Disorders: Official Journal of the Movement Disorder Society*, 18(7), 729–737. <https://doi.org/10.1002/mds.10447>
- Pagonabarraga, J., & Kulisevsky, J. (2012). Cognitive impairment and dementia in Parkinson's disease. *Neurobiology of Disease*, 46(3), 590–596. <https://doi.org/10.1016/j.nbd.2012.03.029>
- Paxinos, G., & Watson, C. (2004). *The rat brain in stereotaxic coordinates—The new coronal set*. Academic Press.
- Perez, M. F., Gabach, L. A., Almiron, R. S., Carlini, V. P., De Barioglio, S. R., & Ramirez, O. A. (2010). Different chronic cocaine administration protocols induce changes on dentate gyrus plasticity and hippocampal dependent behavior. *Synapse*, 64(10), 742–753. <https://doi.org/10.1002/syn.20788>

- Pfeiffer, H. C. V., Løkkegaard, A., Zoetmulder, M., Friberg, L., & Werdelin, L. (2014). Cognitive impairment in early-stage non-demented Parkinson's disease patients. *Acta Neurologica Scandinavica*, *129*(5), 307–318. <https://doi.org/10.1111/ane.12189>
- Pioli, E. Y., Meissner, W., Sohr, R., Gross, C. E., Bezard, E., & Bioulac, B. H. (2008). Differential behavioral effects of partial bilateral lesions of ventral tegmental area or substantia nigra pars compacta in rats. *Neuroscience*, *153*(4), 1213–1224. <https://doi.org/10.1016/j.neuroscience.2008.01.084>
- Rodriguez-Pallares, J., Parga, J. A., Muñoz, A., Rey, P., Guerra, M. J., & Labandeira-Garcia, J. L. (2007). Mechanism of 6-hydroxydopamine neurotoxicity: The role of NADPH oxidase and microglial activation in 6-hydroxydopamine-induced degeneration of dopaminergic neurons. *Journal of Neurochemistry*, *103*(1), 145–156. <https://doi.org/10.1111/j.1471-4159.2007.04699.x>
- Sarkisyan, G., & Hedlund, P. B. (2009). The 5-HT7 receptor is involved in allocentric spatial memory information processing. *Behavioural Brain Research*, *202*(1), 26–31. <https://doi.org/10.1016/j.bbr.2009.03.011>
- Shapira, A. H. V., Chaudhuri, K. R., & Jenner, P. (2017). Non-motor features of Parkinson disease. *Nature Reviews Neuroscience*, *18*(7), 435–450. <https://doi.org/10.1038/nrn.2017.62>
- Schirinzi, T., Madeo, G., Martella, G., Maltese, M., Picconi, B., Calabresi, P., & Pisani, A. (2016). Early synaptic dysfunction in Parkinson's disease: Insights from animal models. *Movement Disorders*, *31*(6), 802–813. <https://doi.org/10.1002/mds.26620>
- Sindhu, K. M., Banerjee, R., Senthilkumar, K. S., Saravana, K. S., Raju, B. C., Rao, J. M., & Mohanakumar, K. P. (2006). Rats with unilateral median forebrain bundle, but not striatal or nigral, lesions by the neurotoxins MPP+ or rotenone display differential sensitivity to amphetamine and apomorphine. *Pharmacology Biochemistry and Behavior*, *84*(2), 321–329. <https://doi.org/10.1016/j.pbb.2006.05.017>
- Tadaiesky, M. T., Dombrowski, P. A., Figueiredo, C. P., Cargnin-Ferreira, E., Da Cunha, C., & Takahashi, R. N. (2008). Emotional, cognitive and neurochemical alterations in a premotor stage model of Parkinson's disease. *Neuroscience*, *156*(4), 830–840. <https://doi.org/10.1016/j.neuroscience.2008.08.035>
- Teyler, T. J., & Discenna, P. (1987). Long-term potentiation. *Annual Review of Neuroscience*, *10*(1), 131–161.
- van Deijk, A. L. F., Camargo, N., Timmerman, J., Hesitek, T., Brouwers, J. F., Mogavero, F., Mansvelder, H. D., Smit, A. B., & Verheijen, M. H. (2017). Astrocyte lipid metabolism is critical for synapse development and function in vivo. *Glia*, *65*(4), 670–682. <https://doi.org/10.1002/glia.23120>
- Vanderschuren, L. J. M. J., Donné Schmidt, E., De Vries, T. J., Van Moorsel, C. A., Tilders, F. J., & Schoffelmeer, A. N. (1999). A single exposure to amphetamine is sufficient to induce long-term behavioral, neuroendocrine, and neurochemical sensitization in rats. *Journal of Neuroscience*, *19*(21), 9579–9586. <https://doi.org/10.1523/jneurosci.19-21-09579.1999>
- Villalba, R. M., & Smith, Y. (2017). Loss and remodeling of striatal dendritic spines in Parkinson's disease: From homeostasis to maladaptive plasticity? *Journal of Neural Transmission*, *125*(3), 431–447. <https://doi.org/10.1007/s00702-017-1735-6>
- Voorn, P., Vanderschuren, L. J. M. J., Groenewegen, H. J., Robbins, T. W., & Pennartz, C. M. (2004). Putting a spin on the dorsal-ventral divide of the striatum. *Trends in Neurosciences*, *27*(8), 468–474. <https://doi.org/10.1016/j.tins.2004.06.006>
- Weintraub, D., Tröster, A. I., Marras, C., & Stebbins, G. (2018). Initial cognitive changes in Parkinson's disease. *Movement Disorders*, *33*(4), 511–519. <https://doi.org/10.1002/mds.27330>
- Williams-Gray, C. H., Evans, J. R., Goris, A., Foltynie, T., Ban, M., Robbins, T. W., Brayne, C., Kolachana, B. S., Weinberger, D. R., Sawcer, S. J., & Barker, R. A. (2009). The distinct cognitive syndromes of Parkinson's disease: 5 year follow-up of the CamPaIGN cohort. *Brain*, *132*(11), 2958–2969. <https://doi.org/10.1093/brain/awp245>
- Yuan, H., Sarre, S., Ebinger, G., & Michotte, Y. (2005). Histological, behavioural and neurochemical evaluation of medial forebrain bundle and striatal 6-OHDA lesions as rat models of Parkinson's disease. *Journal of Neuroscience Methods*, *144*(1), 35–45. <https://doi.org/10.1016/j.jneumeth.2004.10.004>